Simultaneous Inhibition of Entry and Replication of Novel Corona Virus by Grazoprevir: A Computational Drug Repurposing Study

Santosh Kumar Behera,[#][a] Nazmina Vhora,[#][a] Darshan Contractor,[#][a] Amit Shard,[*][b] Dinesh Kumar,[*][b] Kiran Kalia,[*][a] Alok Jain,[*][a]

[a]   Department of Biotechnology
       National Institute of Pharmaceutical Education and Research-Ahmedabad (NIPER-A)
       An Institute of National Importance, Government of India
       Department of Pharmaceuticals, Ministry of Chemicals and Fertilizers,
       Opp. Airforce Station, Palaj, Gandhinagar - 382355, Gujarat, INDIA
       Office Tel: +91 79 66745555, +91 79 66745501; Fax: +91 79 66745560

[b]   Department of Medicinal Chemistry
       National Institute of Pharmaceutical Education and Research-Ahmedabad (NIPER-A)
       An Institute of National Importance, Government of India
       Department of Pharmaceuticals, Ministry of Chemicals and Fertilizers,
       Opp. Airforce Station, Palaj, Gandhinagar - 382355, Gujarat, INDIA
       Office Tel: +91 79 66745555, +91 79 66745501; Fax: +91 79 66745560

ABSTRACT

It is evident from the on-going clinical studies (trials) for coronavirus disease 2019 (COVID-19) that treatment with a single drug is not likely to be sufficient. This, in turn, suggests that the drug acts via inhibition of multiple pathways likely to be more successful and promising. Keeping this hypothesis intact, the present study describes for the first-time, Grazoprevir, an FDA approved anti-viral drug primarily approved for HCV, mediated multiple pathway control *via* synergistic inhibition of viral entry targeting host cell Angiotensin Converting Enzyme 2 (ACE-2)/transmembrane serine protease 2 (TMPRSS2) and viral replication targeting RNA-dependent, RNA polymerase (RdRP). We believe that Grazoprevir either alone or given in combination could be effective therapeutics for treatment of COVID-19 pandemic with a promise of unlikely drug resistance owing to multiple inhibition of eukaryotic and viral proteins.

INTRODUCTION

The global COVID-19 outbreak, by SARS-CoV-2 (2019nCoV), has put the world on a standstill owing to its cross-contamination (transmission)[1]. As per the WHO COVID-19 dashboard (27th May 2020), globally 5,406,282 confirmed cases have been reported with 343,562 associated deaths[2]. Additionally, people's lives around the globe have suffered as a consequence of compulsory quarantines/isolations or restrictions. Such critical and pandemic situation demands immediate therapeutic rescue; however, no proven therapy has been established so far[3]. This causes a shift in the policy "from drug discovery to drug repurposing" and, in this course, *in vitro* or *in silico drug* screening tool identified few clinically proven FDA-approved drugs as a possible treatment for COVID-19[4]. Towards this end, antiviral drugs like remdesivir (RdRP inhibitor), favilavir (RdRP inhibitor), lopinavir (protease inhibitors), ritonavir (protease inhibitors), and antimalarial drugs until recently (chloroquine and hydroxychloroquine) are top candidates presently being repurposed and under clinical trials for the treatment of SARS-CoV-2[5].

SARS-CoV-2, belongs to the subfamily orthocoronavirinae, are relatively large having helical symmetry nucleocapsid with a positive-sense single-stranded RNA genome[6]. The infection begins with the viral entry into the host cell following the ligation of viral spike glycoproteins (S glycoprotein) through the receptor-binding domain (RBD) to the cellular protein (receptor) angiotensin-converting enzyme 2 (ACE2) primed by an enzyme called TMPRSS2 (transmembrane serine protease 2)[7,8]. Once SARS-CoV-2 reaches the host cell, it uncoats to complete the genome transcription and following translation process. The genome replication and transcription occur at cytoplasmic membranes, mediated by the viral replicate, a protein complex encoded by the 20-kb replicase gene. The replicase complex is comprised of 16 viral subunits and a number of cellular proteins (enzymes) including RNA-dependent RNA polymerase (RdRP), RNA helicase, and protease. The final protein packing takes place at the cell membrane and the genomic RNA is incorporated as the mature virus is formed by budding from the internal cell membranes[9,10].

Targeting two or more disease pathways is the mainstay of modern therapy which typically relies on the combinations of two or more separate therapy or therapeutics[11]. However, optimization of the best combinations is generally time-consuming and expensive in the clinical development[12]. In order to streamline combination dosing regimens, the development of molecules with dual or multiple inhibitions capabilities against two or more different classes of the target

would be ideal[13]. Given that ACE-2 / TMPRSS2 (eukaryotic) are critical for the fusion of SARS-CoV-2 with host cells and RdRP (viral protein) is essential for viral RNA synthesis, the simultaneous inhibitions of these enzymatic targets by a single-molecule could be a compelling strategy for the treatment of COVID-19[7]. To the best of our knowledge, the approach of targeting eukaryotic host cell proteins and viral protein via single molecule is an unexplored approach for the COVID-19 therapy. We believe this strategy will be more effective considering the analysis of the results of various ongoing clinical trials (single drug therapy vs combination therapy) and offers unlikeness of drug resistance *via* viral mutation owing to multiple targets inhibition of differential origin. Although naturally occurring molecules like δ-viniferin, myricitrin, nympholide A, afzelin, biorobin, hesperidin, and phyllaemblicin B exhibited a strong binding to SARS-CoV-2 main protease (M[Pro])[14] as well as other targets protein like ACE-2 and RdRP, their direct utilization for COVID-treatment seems poor as these molecules lack details studies including safety profile before getting FDA approval.

Multi-target directed ligands (MTDL's) are the drugs with two or more pharmacophores, which are structurally overlapping, or separated by a spacer, in a single molecule[15]. The use of computational tools revolutionized this approach by predicting the association of ligand(s) with respective receptors. It becomes more relevant if clinically proven FDA approved drugs are considered for the studies[16]. In this context, in a quest to find similar MTDL(s), we ventured into several antiviral drugs already in the market and reported here the computational drug repurposing study for their binding affinity with ACE 2 (host cell), TMPRSS2 (host cell), and RdRP (viral) proteins. Grazoprevir, an azamacrocyclic compound indicated for hepatitis C, appeared to be possessing an optimal binding affinity for these three key proteins. The molecular-dynamic (MD) simulations and conformational analysis predicted the stable interactions of grazoprevir with ACE2 and TMPRSS2 proteins with a promising of the successful therapeutic intervention for COVID-19. We strongly believe that our approach for identification of multi-target-directed USFDA approved drug grazopravir may provide new avenues for the therapeutic management of SARS-CoV-2 infection.

RESULTS AND DISCUSSIONS

Molecular docking study: Grazoprevir interacts with the key residues of ACE2, TMPRSS2, and RdRP

Molecular docking describes the "best-fit" orientation of a ligand to a particular protein. This is fundamentally an optimization problem, which is of high interest in computational studies[17]. To unzip the potential anti-COVID activity among selected 45 ligands (antiviral drugs), molecular interaction along with its conformations in the binding site of the key targeted proteins ACE2 (host cell protein), TMPRSS2 (host cell protein), and RdRP (viral protein), the docking analysis was performed using the Autodock as discussed in the method section.[18]

All the docked conformation of each ligand was ranked according to its binding energy from highest to lowest (see, supplementary Table 1). All the conformations were visualized and analysed. Among 45 ligands, the top ten ligands possessing highest binding energy were selected from each complex for further analysis (Table 1).

Table 1. Binding Energy of top ten ligands to the respective protein.

Sr no.	Drugs	BE (Kcal/mol) (ACE-2)	Drugs	BE (Kcal/mol) (TMPRSS2)	Drugs	BE (Kcal/mol) (RdRp)
1	Paritaprevir	-7.5	Paritaprevir	-12.18	Paritaprevir	-10.87
2	Rilpivirine	-7.42	Asunaprevir	-10.55	**Grazoprevir**	**-9.99**
3	Saquinavir	-7.24	**Grazoprevir**	**-10.15**	Rilpivirine	-8.16
4	Doravirine	-6.96	Nelfinavir	-8.94	Tipranavir	-8.14
5	Pleconaril	-6.5	Delavirdine	-8.72	Rimantadine	-7.73
6	**Grazoprevir**	**-6.32**	Etravirine	-8.18	Delavirdine	-7.66
7	Efavirenz	-6.3	Saquinavir	-8.15	Asunaprevir	-7.35
8	Tipranavir	-6.22	Indinavir	-8.05	Etravirine	-7.12
9	Asunaprevir	-6.18	Amprenavir	-8.03	Pleconaril	-7.01
10	Delavirdine	-6.17	Boceprevir	-7.68	Boceprevir	-6.88

Paritaprevir and grazoprevir were among the top ten ligands which reflected a better binding affinity with all the three target proteins. This is worth mentioning, that despite of better

binding affinity of paritaprevir, grazoprevir was selected for further analysis as it interacts with the key residues of the target proteins (Figure-1, lower panel) that take part in human and virus interaction, the integral component for the proposed anti-COVID activity. In the case of ACE2, grazoprevir interacts with the residue Gln76, forming a H-bond with 2.92 Å while residues Tyr83, Thr27, Phe28, Lys31, Glu35, Leu39, Glu75, Phe72, and Leu79 are involved in hydrophobic interactions. For TMPRSS2, grazoprevir interacts with Ser441 forming a H-bond with 2.94 Å, hydrophobic and other non-covalent interactions with residues Val280, Gln438, Thr459, Ser436, Cys437, Ser460,Cys465, Gly462, Gly464, Trp461, Gln389, and His296. In case of RdRP, it forms the H-bonds with residues Arg553, Arg555, Thr556, Asp623, Arg624 and other non-covalent interactions with the residues Asp452, Tyr455, Ala554, Asp618, Ser682, Ala688, Ser749, Leu758, Asp760, Asp761 respectively as illustrated in Figure-1, upper panel. It is important to mention that most of these residues are critical either for SARS-CoV-2-host interactions and/or the catalytic activity of these proteins[19–21]. Therefore, blocking of these residues by grazoprevir will ultimately affect the virion-host cell interactions and viral replication.
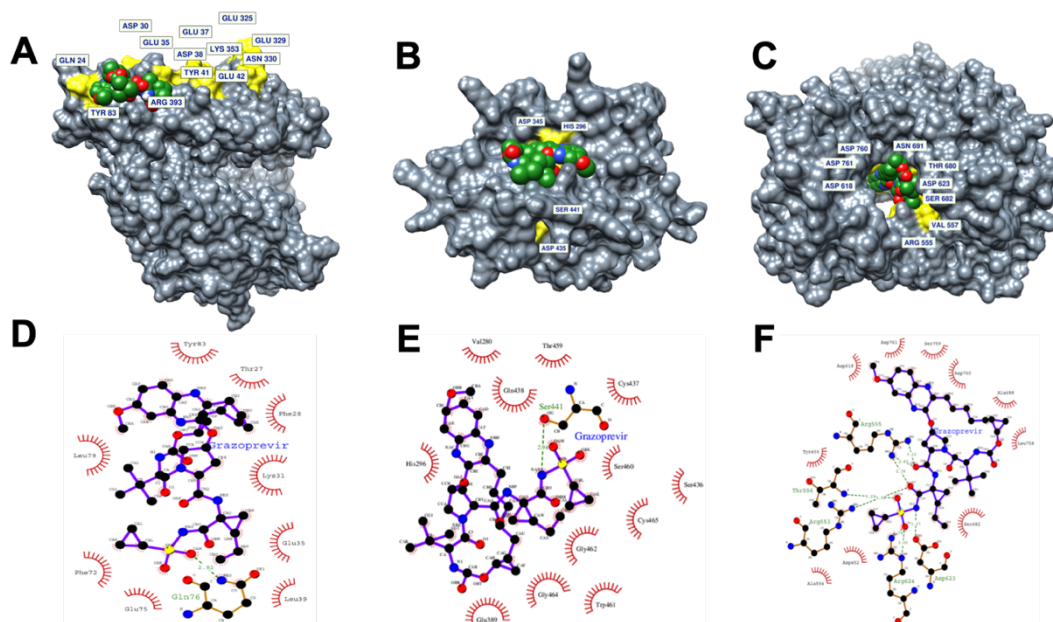

Figure 1. Surface plot and 2D interaction map of protein-ligand interactions of (A, D) ACE2-Grazoprevir (B, E) TMPRSS2-Grazoprevir and (C, F) RdRP-Grazoprevir complexes. Key residues that are reported to critical either for SARS-CoV-2-host interactions and/or the catalytic activity of these proteins are displayed in yellow. Grazoprevir is shown in space filled representation. Ligplot analysis display the hydrogen bond network and the hydrophobic interactions for the docked complexes.

Molecular-dynamic simulations predict stable binding of Grazoprevir to target proteins

Molecular dynamics (MD) is a computer simulation method that helps in analysing the physical movements of several atoms and molecules. For a specific period of time, the atoms and molecules are allowed to interact, representing the dynamic "evolution" of the system[22]. GROMACS simulation package was used for nanosecond-scale molecular dynamics simulations of Apo (only protein) and Holo (Protein-ligand complexes) states of ACE2 and TMPRSS2 as discussed in the method section. To evaluate the stability and behaviour of each system in dynamic environment, the backbone RMSD, RMSF, SASA, intermolecular interactions and PCA were measured from the resultant MD trajectories. The dynamic stability of all the systems, was accessed through RMSD profile of backbone residues that were plotted for 400ns (Figure 2). The backbone RMSD graph of ACE2-Grazoprevir complex (Holo system), reflected a stable trajectory after 250 ns of simulation (Figure 2A) when compared to its Apo state. TMPRSS2-grazoprevir complex reflected an unstable deviation from 50 to 300 ns in comparison to its Apo state which later on reached to a stable state after 300 ns (Figure 2B). The Apo systems of both the targets possess a significant structural deviation in comparison with their holo systems. The ACE2-grazoprevir complex represented a stable RMSD with a value ranging from ~0.3 to ~0.35 nm, whereas TMPRSS2-grazoprevir complex represented a stable value ranging from ~0.45 to ~0.5 nm.
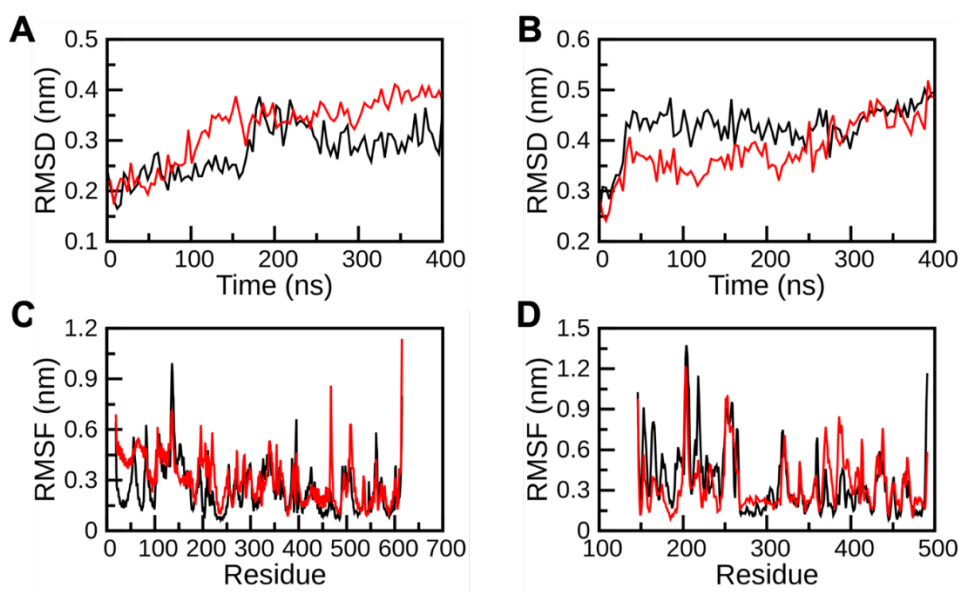

Figure 2. Conformational stability of apo and complex forms of (A, C) ACE2 and (B, D) TMPRSS2 protein. (A, B) Backbone-RMSD and (C, D) Residual RMSF. Profile of apo and complex structures are displayed in red and black lines respectively.

To lineate the results of RMSD graph, Root Mean Square Fluctuation (RMSF) of all the systems were calculated to identify the fluctuation pattern of each residues. The flexibility among the residues in Apo and Holo states of ACE2 and TMPRSS2 was investigated by RMSF of individual residues. The mobility of different residues was observed in all the four systems through RMSF plots (Figure 2). Higher fluctuations were observed in Apo forms than Holo forms which demonstrated the restricted movements throughout the simulation. In Holo state of ACE2, about 10 residues (145-150 and 395-400) exhibited greater deviations in comparison its apo form. Similarly, in case of Holo state of TMPRSS2, about 5 residues (225 to 230) exhibited greater deviations in comparison its apo form. The residual RMSF of binding pocket residues was inferred from each of the complexes and that displayed s the stable nature. The terminal residues from both the ends of the protein were neglected due to their high mobility.

The amino acids of a protein are exposed to certain solvent through hydrophobic interactions. The extent of these interactions with the solvent and the residues at core protein is proportional to the surface area exposed of these environments. In SASA analysis, residues that were shown to important for host-virus interaction[19] or important for the catalytic activity[20] were considered. SASA profile (Figure 3) clearly indicates the decrease in solvent accessible surface in holo states of ACE2 and TMPRSS2 when compared with its Apo states. Fewer accessible areas in Holo states possibly affect the chances of interactions between host and virus as key residues are buried in the complex systems. Subsequently, the results of SASA revealed that the binding of grazoprevir with ACE2 and TMPRSS2 has changed the hydrophilic and hydrophobic areas which may ultimately prevent the host-viral interaction (association). The graphs of ACE2 and TMPRSS2 (Holo states) represented SASA of ~12 nm^2 to ~15 nm^2 and ~0.2 to ~1.5 nm^2 throughout the simulation period which are lesser than Apo states of both the proteins (Figure 3). The SASA results specified that there might be some conformational changes in the protein surface due to which the amino acid residue shifted from the accessible area to buried region and lead to unavailability of binding surface for the virus to human counterpart.
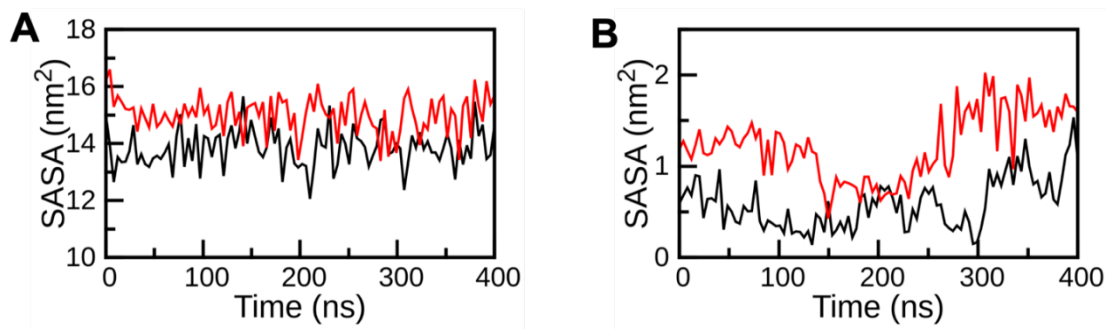
Figure 3. Solvent accessible surface (SASA) analysis of key residues of ACE2 andTMPRSS2 during 400 ns MD Simulations; (A) SASA of ACE2 (B)SASA of TMPRSS2. Complex and apo are displayed by black and red lines respectively.

Generally the stability of a protein and its complexes is based on number of H-bonds and inter molecular interactions. In the present context the total number of hydrogen bonds (intermolecular) was investigated for the Holo systems of ACE2 and TMPRSS2 complex with grazoprevir whose results were depicted in Figure 4A and Fig 4C. The investigation demonstrated a variable number of intermolecular hydrogen bonds in both the complexes throughout the simulation. A cut-off of >10% stable H-bonds and >60% stable contacts were considered for screening of residues with stable H-bonds and other contacts for holo states of ACE2 and TMPRSS2.
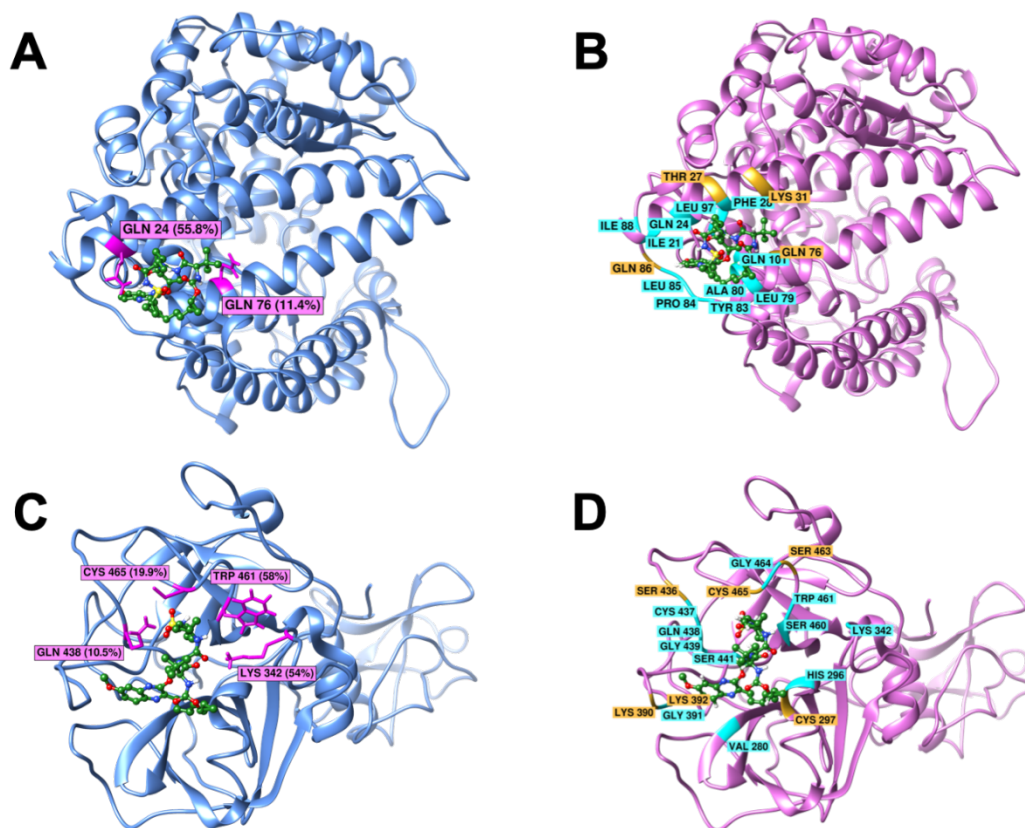
Figure 4. Residues involved in formation of H-bond (A, C) and other non-covalent interactions (B, D) between (A, B) ACE2 and Grazoprevir (C, D) TMPRSS2 and Grazoprevir. Residues forming H-bond that were stable for more than 10% are shown by purple stick in ribbon diagram with respective stability. Other stable non-covalent interactions having more than 80% stability are shown by cyan ribbon. Contacts having 60-80% stability are shown by orange colour. Grazoprevir is shown in ball and stick representation and carbon, oxygen, sulphur and hydrogen atoms are shown in green red, yellow and white colour respectively.

Based on the cut-off score the ACE2-grazoprevir complex represented two H-bonds constituting the residues Gln24 and Gln76 which were found to be stable throughout simulations with 56% and 11% stability (Figure 4A). In addition to the H-bond, the residues Ile21, Gln24, Phe28, Leu79, Tyr83, Pro84, Leu85, Ile88, Leu97 and Gln101 formed the contacts and they were stable for more than 80% of simulation time as depicted in Figure 4B. Besides these other residues namely Thr27, Lys31, Gln76, Gln86 also formed the contact and their stabilities varies from 60-80% simulation time. Subsequently, the analysis of TMPRSS2-grazoprevir complex formed four H-bonds constituting the residues Lys342, Gln438, Trp461and Cys465 which was found to be stable throughout simulations with 56%, 11%, 58%, and 20% stability (Figure 4C). In addition to the H-bond, the residues Val280, His296, Lys342, Gly391, Cys437, Gln438, Gly439, Ser441,

Ser460, Trp461, Gly464, were involved in stable contacts with more than 80% stability (Figure 4D). Other contacts (60-80% stable) were formed by Cys297, Lys390, Lys392, Ser436, Ser463, Cys465. Majority of these interacting residues were hydrophobic/aromatic and it can be interpreted that hydrophobic and π-π interactions make the complex more stable. However, contributions of H-bonds and polar interactions cannot be undermined as they provide the specificity of the ligand-protein binding. It is important to mentioned that many of above-mentioned residues namely Gln24, Thr27, Phe28, Lys31, Leu79, Tyr83 for ACE2 and H296, S441 for TMPRSS2 are reported to critical for host-virus interaction and catalytic activity[19,20]. As they are engaged to form the contacts/interactions with grazoprevir they possibly not available to initiate the viral fusion (ACE2) and further cleavage (TMPRSS2). Additionally, few of these H-bonds and stable contacts were reported for the first time which could explore the antiviral potentiality of Grazoprevir.

To infer the mechanical properties like structural motions and fluctuations of all the states of ACE2 and TMPRSS2, PCA or Essential dynamics (ED) analysis was carried out. A set of eigenvectors was acquired from the MD trajectories which depicted the motion of every solitary component through vectorial depictions

The structural motions or fluctuations of every component within the Apo and Holo states of ACE2 and TMPRSS2 protein were illustrated through first two principal components graphed against EV1 and EV2 (illustrated in Figure 5). The graphs represented higher scattering of components in Apo form in comparison to Holo forms. This specifies a larger conformational change in Holo systems which satisfy the desired MD analysis. The results of PCA analysis in both the cases of the protein-grazoprevir complexes were well correlated with its RMSF analysis (Figure 2).
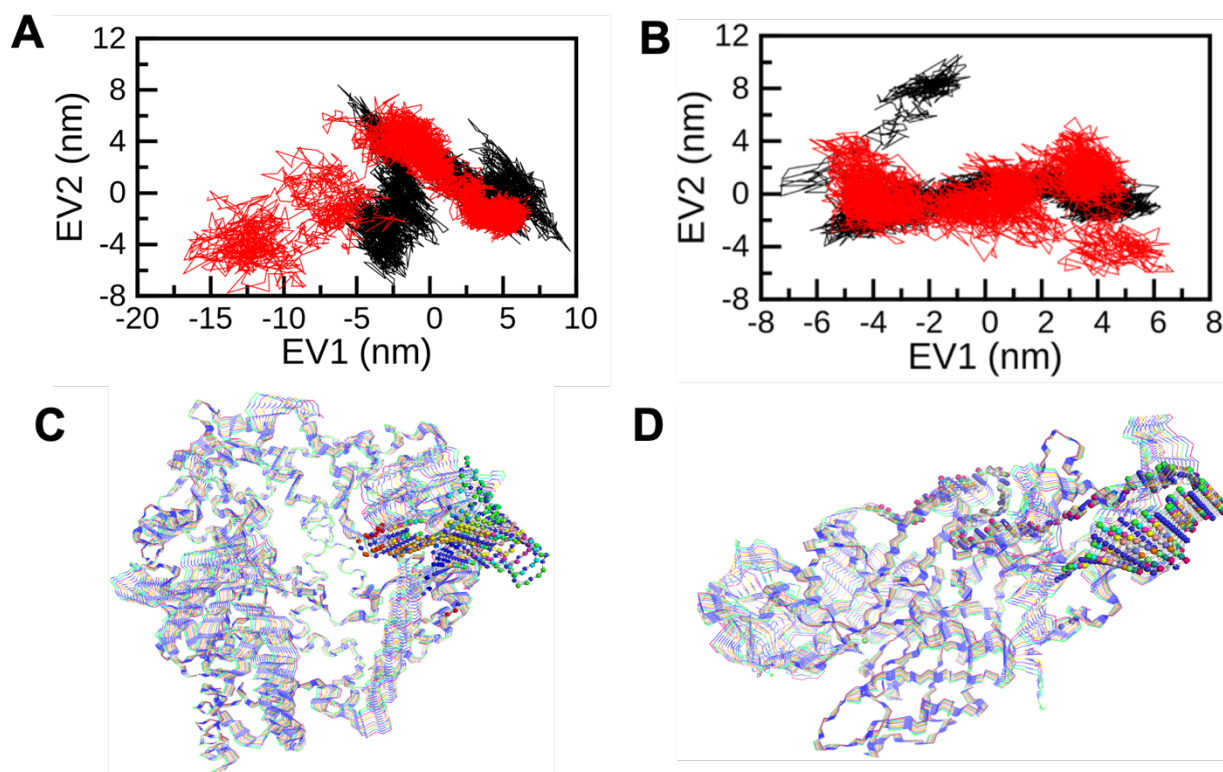
Figure 5. Projection of the motion of the apo and holo forms of ACE2 and TMPRSS2 in phase space along the first two principal eigenvectors (EV1 and EV2) for (A) ACE2 and (B) TMPRSS2. Graphical representation of structures extracted from dynamic trajectories showing prevalent motions in (C) ACE2 and (D) TMRRSS2.

Mostly in every simulation protocol the flexibility of Apo and Holo states were confined and determined by its trace values of the covariance matrix obtained through its diagonalized backbone atoms. The depicted trace values of Apo and Holo state of ACE2 was 59.9 nm^2 and 41.3 nm^2 (see SI Figure S1). Similarly, the trace value of Apo and Holo state of TMPRSS2 were depicted and was found to be 59.9 nm^2 and 36.2 nm^2 (Figure S1). The lower trace values in both the Holo states confirms the overall decreased in flexibility of ACE2 and TMPRSS2 compared to their Apo forms.

The fluctuations or structural motions of the components in the system were well analysed through correlating the graph and trajectory analysis. The dynamic trajectories that were obtained from EV1 of ACE2 and TMRRSS2 (Figure 5C and 5D) has represented a fluctuation pattern of amino acid residues in each system which were identified by superimposition of the 100 confirmations with an interval of 10. Most of the residues are seemed to be fluctuated but the residues 131-141 in ACE2 and 227-237 in TMPRSS2 (represented in ball in stick model 5C and 5D) were observed to have more mobile regions and may get exposed then others. This depicts

that the residues considered in the investigation of SASA were found to have less mobility which may be due to strong interactions between protein-grazoprevir complexes. The results of this analysis could be well aligned with the results of SASA.

In the current investigation an integrative approach was performed where the techniques of docking, homology modelling and MD simulations was employed. This approach could able to explore the residual movements, and its key interactions which are not only confined with the intra-molecular but also the intermolecular ACE2 and TMPRSS2 interactions with grazoprevir. Furthermore this study could able to unzip the association between the movements of residues in the ACE2 and TMPRSS2 Apo and Holo states trajectories. The results from this investigation could able to signify the potentiality of grazoprevir for antiviral therapeutics. Thus, following the multiple computational approaches, we envisage that grazoprevir could be repurposed for fighting against the COVID-19 pandemic. As predicted, grazoprevir interacts with all three proteins (host cell as well as virion) optimally with stable binding conformations. Since, this drug, grazoprevir, is marketed as fixed-dose combinations with elbasvir (Zepatier™), which was also reported to have anti-COVID activity recently[23]. Thus, it is encouraging for effective drug combinations to derive their synergistic effects. The propensity of grazoprevir to bind fundamentally different eukaryotic and SARS-CoV-2 proteins with strong affinities remain unexplained. However, the contribution from the drug's structural and geometric dimensions leading to polar atoms oriented electrostatic interactions with target proteins cannot be ruled out in additional to various covalent and H-bonding interactions.

CONCLUSIONS

Following multi-target directed ligands (MTDL's) screening, we disclose grazoprevir exhibits optimal affinity for the key proteins engaged in viral entry into host cells (ACE2 and TMPRSS2) and its replication (RdRP) assembling new virions as predicted by molecular docking, homology modeling, and molecular simulations (MD) studies. We therefore propose clinical tests of grazoprevir as a therapeutic drug for the COVID-2 alone to its combination with elbasvir as Zepatier.™ We believe the strategy of targeting host-cell proteins and virion protein simultaneously by a single molecule for COVID-19 therapy will not only improve the patient

compliance but also minimize the side effects due to dose reduction, likely drug resistance owing to multiple pathway inhibition, and cost of therapy.

MATERIAL AND METHODS

Selection of protein, Structure retrieval and prediction

Three proteins namely Angiotensin Converting Enzyme-2 (ACE2), Transmembrane protease serine 2 (TMPRSS2) and RNA-dependent RNA polymerase (RdRP) (viral protein) were chosen for this investigation. All these proteins play a key role in COVID-19 (SARS-CoV-2 infections) pathophysiology, particularly, host cell entry and viral RNA replication. The three dimensional structure of ACE2 and RdRP was retrieved from Protein Data Bank[24] (http://www.rcsb.org/pdb/home.do) with PDB ID: 6M0J[20] and 7BTF.[21] The co-crystallized Receptor Binding domain (RBD) of spike protein from ACE2 and the co-crystallized cofactors nsp7 and nsp8 of RdRP were separated through BIOVIA Discovery Studio 4.5 Visualizer[25] or UCSF Chimera.[26] The non-interacting ions, all water molecules were removed before the docking. The missing hydrogen atoms were added using UCSF Chimera 1.13, an extensible molecular modelling program. [26]

The three-dimensional structure of TMPRSS2 protein was generated by SWISS-MODEL online server using the amino acid sequence from UniProt (UniProt KB-O15393) due to non-availability of its crystal structure. Serine protease hepsin's (PDB: 5CE1) structure was selected as a template which was having highest sequence identity amongst more than 50 templates available, that was 33.82% using the similar protocol as discussed elsewhere.[19,27] Modelled structure (residues 146-491) included the peptidase S1 domain that is important for its catalytic activity. 92% residues are within the allowed regions according to the Ramachandran Plot. The modelled TMPRSS2 protein was cross validated for its structural coordinates using computational methods.

SARS-CoV-2 RdRP with 942 amino acids was directed for domain search for recognizing the key region of the protein for further analysis. Based on the studies of Gao *et al*., 2020 it was understood that the structure of the 2019 novel corona virus (2019-nCoV) nsp12 is composed of a "right hand" RdRP domain (residues S367-F920). This RdRP domain constitutes a well conserved polymerase domain having three subdomains namely fingers subdomain (L366-A581 and K621-

G679), a palm subdomain (T582-P620 and T680-Q815), and a thumb subdomain (H816-E920). Considering the above statements, the RdRP protein with residues from 367 to 932 was selected for further computational analysis.

The binding site of the ACE2, TMPRSS2 and RdRp were identified by taking together the consensus results of CASTp (Computed Atlas of Surface Topography of Proteins), RBD of spike protein binding site (for ACE2), catalytic site (for TMPRSS2) and remdesivir binding site (for RdRp).

Ligand selection and preparation

Clinically proven Food and Drug Administration (FDA) approved 45 anti-viral drugs were considered in the current investigation. The sdf format of all the 45 inhibitors were retrieved from NCBI PubChem database. This .sdf file were converted into pdb through Online SMILES (Simplified Molecular Input Line Entry System) translator web server (https://cactus.nci.nih.gov/translate/) or Open Babel GUI was used to convert or PDBQT format towards input to AutoDock 4.2 (autodock.scripps.edu/) docking tool[28].

Molecular docking

Molecular docking investigations were carried out for ACE2, TMPRSS2, and RdRp protein against all the 45 drugs using AutoDock 4.2. AutoDock Tools (ADT) v.1.5 was used for assigning Kollman charges for protein and Geister partial charges for all the 45 ligands. To permit full-extended conformation of ligand, different grid values were chosen for all the three proteins with a particular dimension space, and parameters based on x-centering:, y-centering:, and z-centering. Residues that are involved in binding of spike protein (for ACE2), or catalytic activity (for TMPRSS2 and RdRP) were selected for grid generation as illustrated in Figure 1. Grid box was observed to cover all the selected residues. The best docking conformation was calculated by using the Lamarckian Genetic Algorithm (LGA).The best resultant docked complexes were selected based on binding energy, and intermolecular interactions between ligand and protein covering most of the residues shown in Figure 1. The best docking complexes from each system were screened from the independent molecular docking for further analysis. Lig-Plot+[29], UCSF-Chimera[26]and Biovia Discovery Studio Visualizerv4.5[25]were used for image generation and protein-ligand interaction analysis.

Molecular Dynamics (MD) simulations

The MD simulations were carried out for the Apo and Holo systems of ACE2, and TMPRSS2 using GROMOS 54A7 force-field [30] using GROMACS suit (version 2019.4)[31] to understand the dynamic behaviour, approach of binding and inhibitor specificity for all the systems. The protein-ligand complex structure was considered from the final docked structures as discussed above. Automated Topology Builder (ATB)[32] was used for generation of force-field parameters of Grazoprevir . The initial structure was solvated using the extended SPC water model[33]. All the systems were immersed in a cubic box of SPC/E water molecules with minimum distance of 12 Å between the protein surface and the edge of the box. The solvated system was neutralized by adding a counterions. Energy minimization was performed for releasing the conflicting contacts, using the steepest descent method with a tolerance of 10 kJ mol^{-1}. Energy minimized systems were subjected to equilibration phase-I in which all the heavy atoms were position restrained for 2 ns in NVT ensemble. Further, followed by the secondary phase in NPT ensemble for 2 ns. All the systems were kept at constant 300 K in association with the velocity-rescale thermostat[34] with a coupling constant 0.1 ps. During the 400 ns production run Parrinello-Rahman coupling algorithm[35] was used for keeping the pressure constant at 1 bar with a coupling constant of 2 ps. Particle Mesh Ewald method[36] with a cut-off of 1.4 nm was used for evaluation of long range non-bonded interactions in the systems and van der Waals interactions. Periodic boundary conditions were applied in all three (x, y, z) directions. All the bonds length were constrained using LINCS algorithm.[37] SETTLE algorithm[38] was used to constrain the geometry of water molecules. The trajectories of MD simulations were analysed by inbuild modules of Gromacs or inhouse scripts. Root Mean Square Deviation (RMSD), Root Mean Square Fluctuation (RMSF), Solvent Accessible Surface Area (SASA) of key interacting residues, Principal Component Analysis (PCA) and stability of various non-covalent interactions were analysed. A sphere of water molecules was used to calculate the SASA[39] of molecules. Stability of non-covalent interactions were measured by *gmx_hbond*, *gmx_mindist* and in-house scripts. Contacts were defined if minimum distance between any atoms of protein residues and ligand was between 0.4nm. PCA was carried out through essential dynamics (ED) method using *gmxcovera* and *gmxaneig* modules of Gromacs simulation suit. A set of eigenvectors and eigenvalues were obtained after diagonalzing and calculating the covariance matrix which reflects concerted motion of the

molecules. In the present investigation, the first two Principal Components (PCs) i.e PC1 and PC2, which dominate the collective motions in Apo and Holo forms were considered for further analysis. All 2D plots were generated by GNU plot for data analysis.

REFERENCES

1. Kupferschmidt, K. & Cohen, J. Will novel virus go pandemic or be contained? *Science* **367**, 610–611 (2020).

2. Coronavirus Disease (COVID-2019) Situation Reports. (2019). Available at: https://www.who.int/emergencies/diseases/novel-coronavirus-2019/situation-reports.

3. Morse, J. S., Lalonde, T., Xu, S. & Liu, W. R. Learning from the Past: Possible Urgent Prevention and Treatment Options for Severe Acute Respiratory Infections Caused by 2019-nCoV. *ChemBioChem* **21**, 730–738 (2020).

4. "Repurposing Drugs'. National Center for Advancing Translational Sciences (NCATS). U.S. Department of Health & Human Services, National Institutes of Health,". (2020). Available at: https://ncats.nih.gov/preclinical/repurpose.

5. Harrison, C. Coronavirus puts drug repurposing on the fast track. *Nature biotechnology* **38**, 379–381 (2020).

6. de Groot, R. J. *et al.* Coronaviridae. in *Virus Taxonomy* 806–828 (Elsevier, 2012). doi:10.1016/B978-0-12-384684-6.00068-9

7. Hoffmann, M. *et al.* SARS-CoV-2 Cell Entry Depends on ACE2 and TMPRSS2 and Is Blocked by a Clinically Proven Protease Inhibitor. *Cell* **181**, 271-280.e8 (2020).

8. Du, L. *et al.* The spike protein of SARS-CoV - A target for vaccine and therapeutic development. *Nature Reviews Microbiology* **7**, 226–236 (2009).

9. Ziebuhr, J. The coronavirus replicase. *Current Topics in Microbiology and Immunology* **287**, 57–94 (2005).

10. Lai, M. M. & Cavanagh, D. The molecular biology of coronaviruses. *Adv. Virus Res.* **48**, 1—100 (1997).

11. Bang, S., Son, S., Kim, S. & Shin, H. Disease Pathway Cut for Multi-Target drugs. *BMC Bioinformatics* **20**, 1–12 (2019).

12.   Kaur, G. Polypharmacy: The past, present and the future. *J. Adv. Pharm. Technol. Res.* **4**, 224–225 (2013).

13.   Zhou, J. *et al.* Rational Design of Multitarget-Directed Ligands: Strategies and Emerging Paradigms. *J. Med. Chem.* **62**, 8881–8914 (2019).

14.   Joshi, R. S. *et al.* Discovery of potential multi-target-directed ligands by targeting host-specific SARS-CoV-2 structurally conserved main protease. *J. Biomol. Struct. Dyn.* 1–16 (2020).

15.   Sucharita Das and Soumalee Basu. *Strategies for Multi-Target Directed Ligands: Application in Alzheimer's Disease (AD) Therapeutics. In: Roy K. (eds). Multi-Target Drug Design Using Chem-Bioinformatic Approaches. Methods in Pharmacology and Toxicology. Humana Press, New York, NY* (2018).

16.   Ramsay, R. R., Popovic-Nikolic, M. R., Nikolic, K., Uliassi, E. & Bolognesi, M. L. A perspective on multi-target drug discovery and design for complex diseases. *Clin. Transl. Med.* **7**, (2018).

17.   Vijesh, A. M., Isloor, A. M., Telkar, S., Arulmoli, T. & Fun, H. K. Molecular docking studies of some new imidazole derivatives for antimicrobial properties. *Arab. J. Chem.* **6**, 197–204 (2013).

18.   Pantsar, T. & Poso, A. Binding Affinity via Docking: Fact and Fiction. *Molecules* **23**, 1899–1900 (2018).

19.   Meng, T. *et al.* The insert sequence in SARS-CoV-2 enhances spike protein cleavage by TMPRSS. *bioRxiv* 2020.02.08.926006 (2020). doi:10.1101/2020.02.08.926006

20.   Lan, J. *et al.* Structure of the SARS-CoV-2 spike receptor-binding domain bound to the ACE2 receptor. *Nature* **581**, 215–220 (2020).

21.   Gao, Y. *et al.* Structure of the RNA-dependent RNA polymerase from COVID-19 virus. *Science (80-.).* **368**, 779–782 (2020).

22.   Jacob D Durrant and J Andrew McCammon. Molecular dynamics simulations in drug discovery. *BMC Biol.* **9**, 1–9 (2011).

23.   Balasubramaniam, M. & Shmookler Reis, R. Computational Target-Based Drug Repurposing of Elbasvir, an Antiviral Drug Predicted to Bind Multiple SARS-CoV-2

Proteins. (2020). doi:10.26434/CHEMRXIV.12084822.V2

24.   Goodsell, D. S. *et al.* RCSB Protein Data Bank: Enabling biomedical research and drug discovery. *Protein Sci.* **29**, 52–65 (2020).

25.   BIOvIA, D. S. (2015). Discovery studio modeling environment. San Diego, Dassault Systemes, Release, 4. 2015 (2015).

26.   Pettersen, E. F. *et al.* UCSF Chimera - A visualization system for exploratory research and analysis. *J. Comput. Chem.* **25**, 1605–1612 (2004).

27.   Sourav, P. & Dr. Arindam, T. Compilation of Potential Protein Targets for SARS-CoV-2: Preparation of Homology Model and Active Site Determination for Future Rational Antiviral Design. *chemRxiv* (2020). doi:10.26434/chemrxiv.12084468.v1

28.   Morris, G. M. *et al.* AutoDock4 and AutoDockTools4: Automated Docking with Selective Receptor Flexibility. *J. Comput. Chem.* **30**, 2785–2791 (2009).

29.   Roman A. Laskowski*, † and Mark B. Swindells‡. LigPlot+: Multiple Ligand–Protein Interaction Diagrams for Drug Discovery. *J. Chem. Inf. Model.* **51**, 2778–2786 (2011).

30.   Schmid, N. *et al.* Definition and testing of the GROMOS force-field versions 54A7 and 54B7. *Eur. Biophys. J.* **40**, 843–856 (2011).

31.   Abraham, M. J. *et al.* GROMACS: High performance molecular simulations through multi-level parallelism from laptops to supercomputers. *SoftwareX* **1–2**, 19–25 (2015).

32.   Stroet, M. *et al.* Automated Topology Builder Version 3.0: Prediction of Solvation Free Enthalpies in Water and Hexane. *J. Chem. Theory Comput.* **14**, 5834–5845 (2018).

33.   Mark, P. & Nilsson, L. Structure and dynamics of the TIP3P, SPC, and SPC/E water models at 298 K. *J. Phys. Chem. A* **105**, 9954–9960 (2001).

34.   Berendsen H.J.C., Postma J.P.M., van Gunsteren W.F., H. J. *Interaction Models for Water in Relation to Protein Hydration. Springer, Dordrecht* **14**, (1981).

35.   Bussi, G., Donadio, D. & Parrinello, M. Canonical sampling through velocity rescaling. *J. Chem. Phys.* **126**, (2007).

36.   Parrinello, M. & Rahman, A. Polymorphic transitions in single crystals: A new molecular dynamics method. *J. Appl. Phys.* **52**, 7182–7190 (1981).

37.   Essmann, U. *et al.* A smooth particle mesh Ewald method. *J. Chem. Phys.* **103**, 8577–8593 (1995).

38.   Hess, B., Bekker, H., Berendsen, H. J. C. & Fraaije, J. G. E. M. LINCS: A Linear Constraint Solver for molecular simulations. *J. Comput. Chem.* **18**, 1463–1472 (1997).

39.   Gerlt, J. A., Kreevoy, M. M., Cleland, W. W. & Frey, P. A. Understanding enzymic catalysis: The importance of short, strong hydrogen bonds. *Chem. Biol.* **4**, 259–267 (1997).

AUTHOR CONTRIBUTIONS: KK, AJ, DK, and AS conceptualized the proposed work. AJ, SKB, NV, DC performed all the computation studies. All the authors discussed the various results and wrote the manuscript.

COMPETING INTERESTS: Author declares no competing results

ADDITIONAL INFORMATION: Supplementary information is available for this paper at https://doi.org/xx

AUTHOR INFORMATION & CORRESPONDENCE

[#]All the authors contribute equally
Corresponding Author
Dr. Alok Jain (Email: alokjain@niperahm.ac.in, alokjain16@gmail.com)

Co-Corresponding Authors

Prof. Kiran Kalia (Email: director@niperahm.ac.in, kirankalia@gmail.com)
Dr. Dinesh Kumar (Email: dkchem79@gmail.com)
Dr. Amit Shard (Email: amit@niperahm.ac.in)